

Distinctive effects of interplanetary electric field and substorm on nighttime equatorial F layer: A case study

D. Chakrabarty,¹ R. Sekar,¹ J. H. Sastri,² and Sudha Ravindran³

Received 21 July 2008; revised 1 September 2008; accepted 5 September 2008; published 11 October 2008.

[1] A geomagnetic storm event is identified wherein the base of the equatorial F layer ($h'F$) over dip equator moved unusually upward till premidnight hours and descended thereafter. The $h'F$ variation is linearly correlated with the variation in the smoothed auroral electrojet index (AE) which varies slowly. The fast fluctuations (residuals) with periodicity ~ 42 min in the vertical plasma drift are found to be causally related with the fast fluctuations in the dawn-to-dusk component of interplanetary electric field (IEFy) and interestingly, not with the fast fluctuations in AE. However, during the interval when a substorm was triggered in association with sharp transitions in IEFy polarity, the drift fluctuations follow the AE fluctuations and are out of phase with IEFy fluctuations. The investigation demonstrates distinctive effects of IEFy and substorm-related current systems on the zonal electric field over dip equator in the premidnight hours during geomagnetic storms.
Citation: Chakrabarty, D., R. Sekar, J. H. Sastri, and S. Ravindran (2008), Distinctive effects of interplanetary electric field and substorm on nighttime equatorial F layer: A case study, *Geophys. Res. Lett.*, 35, L19108, doi:10.1029/2008GL035415.

1. Introduction

[2] It is well-known that the F region vertical plasma drift corresponding to zonal electric field over dip equator changes from upward to downward direction during post-sunset hours. However, this transition, in general, takes place via an intermediate condition when the zonal electric field gets enhanced prior to the reversal. This pre-reversal enhancement (PRE) of zonal electric field lifts the F layer to higher altitudes and in the presence of a rapidly depleting E layer at the bottom, favors the occurrence of Equatorial Spread F (ESF) irregularities [e.g., *Sekar and Kelley*, 1998, *Fejer et al.*, 1999]. *Scherliess and Fejer* [1999] brought out the variations in the magnitude of PRE with solar cycles. Morphological studies by *Subbarao and Krishna Murthy* [1994] indicate that PRE of zonal electric field over Indian zone occurs at ~ 1900 IST (Indian Standard Time, IST = Universal Time, UT + 5.5 hr) during equinoctial months under geomagnetically quiescent conditions irrespective of solar epoch. However, during geomagnetic storms and/or substorms, the zonal electric field over equatorial region may get significantly affected [e.g., *Reddy et al.*, 1979;

Sastri, 2002; *Kelley et al.*, 2003] by interplanetary electric field (IEF) and/or substorm. Although a few aspects of these effects have been addressed based on spectral investigations [e.g., *Earle and Kelley*, 1987; *Chakrabarty et al.*, 2005; *Nicolls et al.*, 2007], explicit attempt has not been made to delineate the effects of IEFy (storm) and substorm-related perturbations on the equatorial F region zonal electric field when both storm and substorm are present simultaneously. In the present communication, one such event is chosen and the effects due to storm and substorm on the F region zonal electric field over dip equator are brought out based on spectral investigations.

2. Results

[3] Figure 1a depicts the $h'F$ ascent (circles joined by line) over Thumba (8.7°N , 77.0°E , dip angle 0.5°N) on March 21, 1998 ($A_p = 35$ on this day after five quiet days) during 1600 hr to 2130 IST by ~ 250 km (from ~ 220 km to ~ 470 km) and subsequently, faster descent after 2130 IST to come back to ~ 220 km by midnight (also referred as 2400 IST). This variation in $h'F$ during 1930–2400 IST is distinctly different from the mean variation (thick solid line) of $h'F$ derived from six quiet days of the month. Note that the variation of $h'F$ slightly deviates from the mean quiet day variation during 1600–1800 IST and, very prominently, during the interval 1930–2330 IST. The temporal variations of auroral electrojet indices, AE (stars joined by line), that assimilated magnetic data from 12 stations in the auroral region, are presented in Figure 1b. As the stations are unevenly spaced and limited in number, magnetic events longitudinally localized and/or latitudinally outside the AE station network, may go undetected [see *Gjerloev et al.*, 2004, and references therein]. The smoothed (slowly varying component) AE variation (thin solid line) obtained by Savitzky-Golay (SG) smoothing algorithm [*Savitzky and Golay*, 1964] during 1600–2400 IST are also superimposed on the AE variation shown in Figure 1b. The advantage of SG algorithm is its ability to suppress the noise with less distortion. It is noted that the temporal variation of the smoothed AE closely follows the $h'F$ variation during 1800–2130 IST. The concurrent reduction in $h'F$ altitude and AE from 2130 IST till ~ 2300 IST is also striking. A linear regression analysis of the smoothed AE curve with the $h'F$ variation during 1800–2300 IST yields high correlation coefficient ($r = 0.89$). Though range ESF was present over Thumba during 2000–2400 IST and as the ionogram traces at low frequencies are rather well-defined, $h'F$ variation during this period is fairly reliable. In order to additionally verify, the measured OI 630.0 nm airglow intensity variations on this night (grey curve, Figure 1c) over Waltair (17.7°N , 83.3°E , dip angle 20°N) [*Taori et al.*,

¹Physical Research Laboratory, Navrangpura, Ahmedabad, India.

²Solar-Terrestrial Physics, Indian Institute of Astrophysics, Bangalore, India.

³Space Physics Laboratory, Vikram Sarabhai Space Center, Thiruvananthapuram, India.

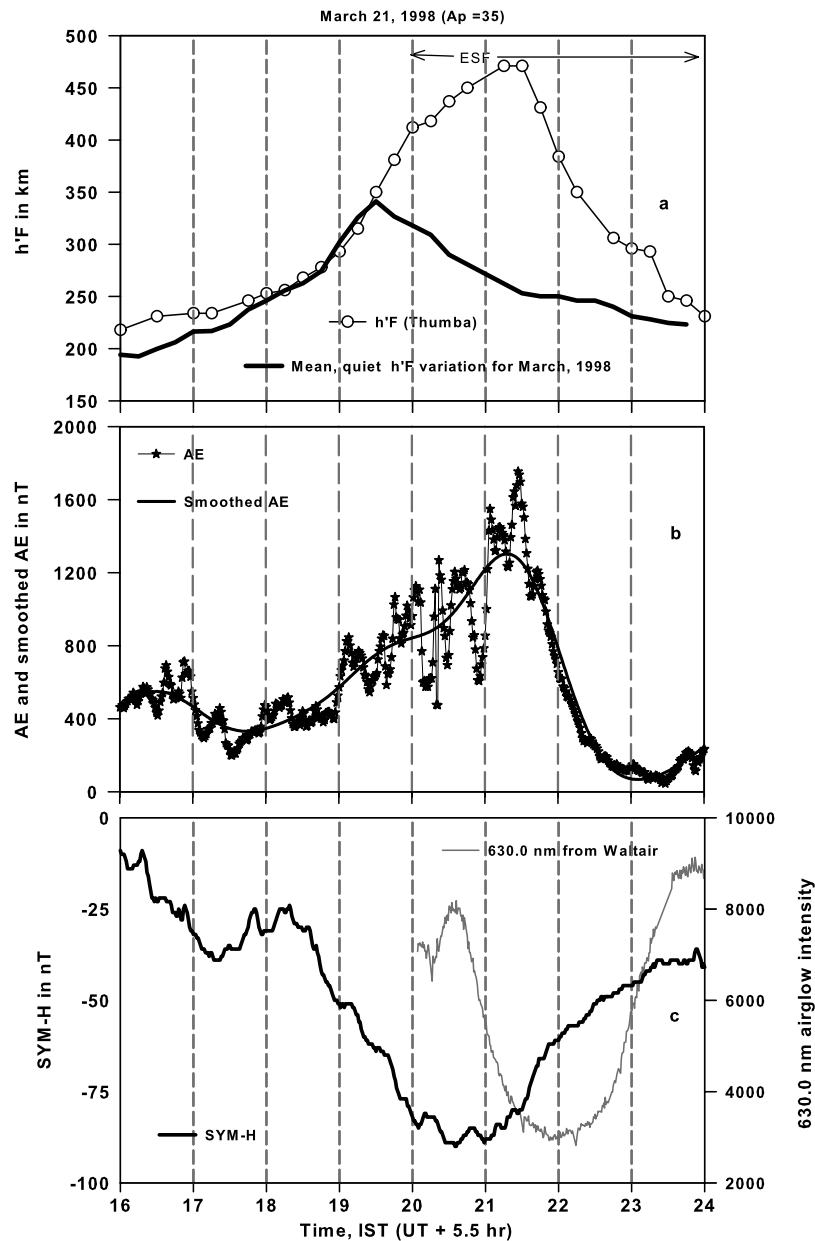


Figure 1. (a) $h'F$ variation over Thumba on March 21, 1998 during 1600–2400 IST compared with the mean, quiet $h'F$ variations, (b) AE and smoothed AE variations, and (c) OI 630.0 nm airglow intensity variation recorded from Waltair and SYM-H variation.

2001] is compared with the $h'F$ variation over equator. The comparison reveals that the variations in $h'F$ and airglow intensity are more or less inversely correlated even though the ionospheric and airglow measurements are made from dip equator and low latitude respectively. Figure 1c also depicts the SYM-H variation revealing the main phase of a geomagnetic storm till 2030 IST followed by recovery phase. An additional sub-recovery phase is also noticed during 1720–1820 IST. It is interesting to note that the ascent of $h'F$ continued even after the main phase of the storm.

[4] Figure 2a depicts the temporal variation of the propagation lag corrected [Chakrabarty *et al.*, 2005] IEFy during 1600–2400 IST, based on the measurements by the Advanced Composition Explorer (ACE) satellite. It is

noted that IEFy turns in the direction of dusk-to-dawn at ~ 1700 IST, dawn-to-dusk at ~ 1730 IST and dusk-to-dawn at ~ 2130 IST. It is also additionally verified based on ACE measurements that the changes in the solar wind velocity during these times are nominal and the rapid changes in IEFy mentioned above are primarily due to the polarity reversals in the Z-component of Interplanetary Magnetic field (IMF Bz). After 2130 IST, IEFy becomes weak and oscillatory till 2300 IST. The variation in ASY-H, which is superimposed on Figure 2a, reveals episodic intensifications centered at ~ 1700 IST and 2130 IST. Figure 2b consists of four subplots depicting the geomagnetic X-component variations at four stations (Muntinlupa, MUT: 3.58°N , 191.57°E ; Lunping, LNP: 13.8°N , 189.5°E ; Rikubetsu, RIK: 34.7°N , 210.8°E ; Tixie, TIX: 65.67°N , 196.88°E)

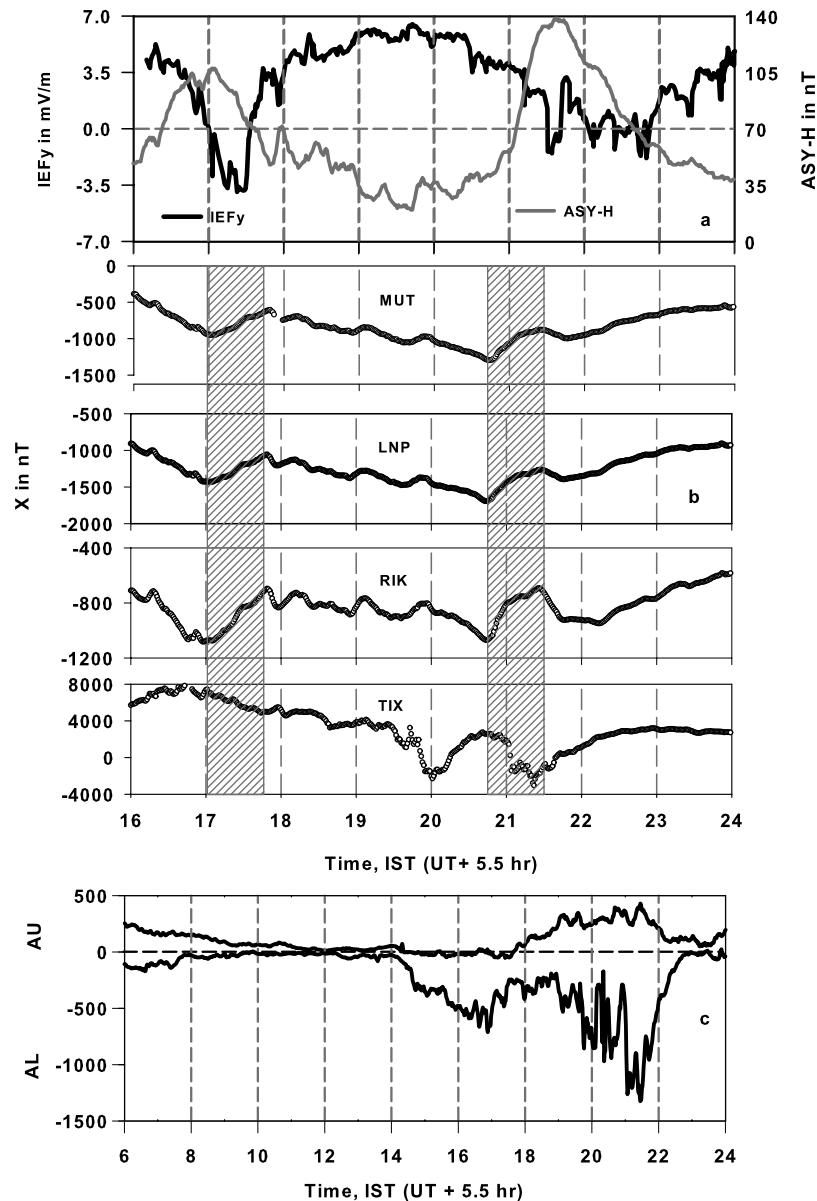


Figure 2. (a) Propagation lag corrected IEFy variation and ASY-H variation during 1600–2400 IST, (b) geomagnetic X component variations at four stations (Muntinlupa, MUT: 3.58°N, 191.57°E; Lunping, LNP: 13.8°N, 189.5°E; Rikubetsu, RIK: 34.7°N, 210.8°E; Tixie, TIX: 65.67°N, 196.88°E) along nearly the same magnetic meridian in the midnight sector. The shaded vertical boxes during 1700–1740 IST and 2040–2130 IST indicate the presence of bay disturbances, and (c) AL and AU variations.

along nearly the same magnetic meridian [Yumoto and the CPMN group, 2001] in the midnight sector. Positive bay disturbances (hatched boxes) are observed at MUT, LNP, RIK starting at ~ 1700 and 2040 IST. At the same intervals, negative bay disturbances are observed at TIX. The temporal variation in AL indices (westward auroral electrojet) in Figure 2c indicates auroral electrojet activity starting at ~ 1400 IST and explosively after ~ 2040 IST after a prolonged quiet interval. The bay disturbances and the auroral electrojet activity start weakening after ~ 2130 IST.

[5] In Figure 3a, temporal variation in IEFy (solid line in grey) during 1900–2400 IST along with a smoothed curve based on SG algorithm (dashed line in grey) are shown. Vertical plasma drift (circles joined by black line) over the magnetic equator based on h/F variation and corrected for

chemical recombination effect is plotted in Figure 3b along with the corresponding smoothed curve (dashed line in grey) based on SG algorithm. The drift values have maximum uncertainty of $\sim \pm 6$ m/s. It is seen that the vertical drift is close to zero at ~ 2145 IST. Based on the respective smoothed curves, the fast fluctuations (residuals) in IEFy and drift are extracted. As the temporal resolution (64 s) of IEFy time series is almost 15 times higher than that of the drift time series, the IEFy residuals (in grey) are smoothed for 15 points and compared with the drift residuals (circles joined by black line) in Figure 3c. It may be noticed that the changes in both the residuals agree well except during 2110–2200 IST (marked by cross-hatched lines) when IEFy flips from dawn-to-dusk to dusk-to-dawn direction in a very short duration. The residuals in IEFy and drift are anti-

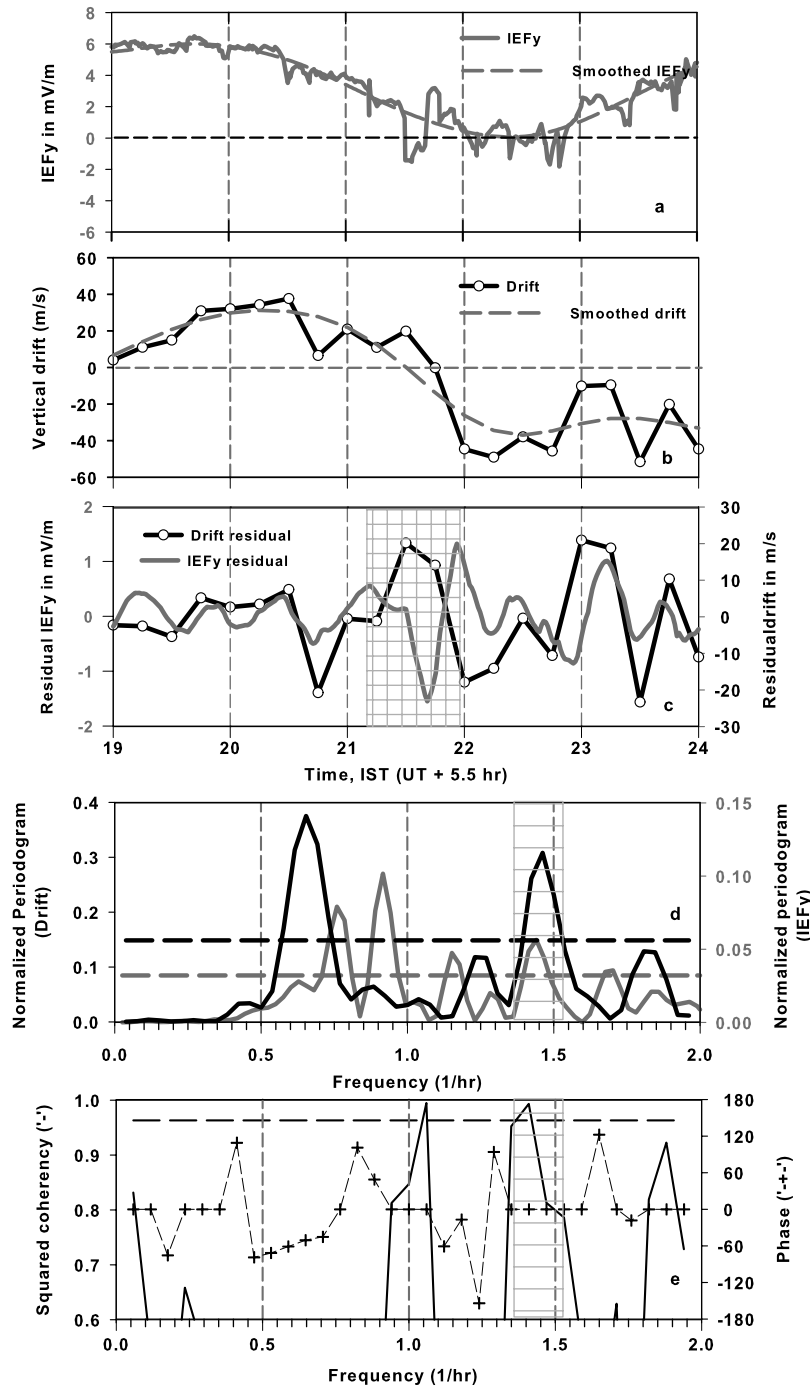


Figure 3. (a) IEFy and smoothed IEFy during 1900–2400 IST. (b) Drift and smoothed drift during the same period. (c) Comparison of the residuals of IEFy and drift. The shaded vertical box reveals the out-of-phase variations of IEFy and drift residuals during 2110–2200 IST. (d) Normalized periodograms for IEFy and drift residuals revealing the harmonic components. (e) Coherency and phase spectra.

correlated during this time. The harmonic components in the drift and IEFy residuals are determined using a standard algorithm [Schulz and Stattegger, 1997]. Figure 3d reveals the harmonic components in the vertical plasma drift (black line) and IEFy (grey line) residuals. It is found that frequency component ~ 1.45 cycles/hr (period ~ 42 min) is present in both the residual drift and IEFy time series and is “significant” (above the respective critical levels deter-

mined by Siegel’s test). In order to establish the causal relationship, if any, between the residual drift and IEFy time series, bivariate spectral analysis [Schulz and Stattegger, 1997] is performed and the outcome is shown in Figure 3e. The analysis reveals that the coherency (solid line) is significantly (above the False Alarm Level depicted by dashed line) high for the frequency components ~ 1.0 cycle/hr (period 1.0 hr) and 1.45 cycles/hr (period ~ 42 min).

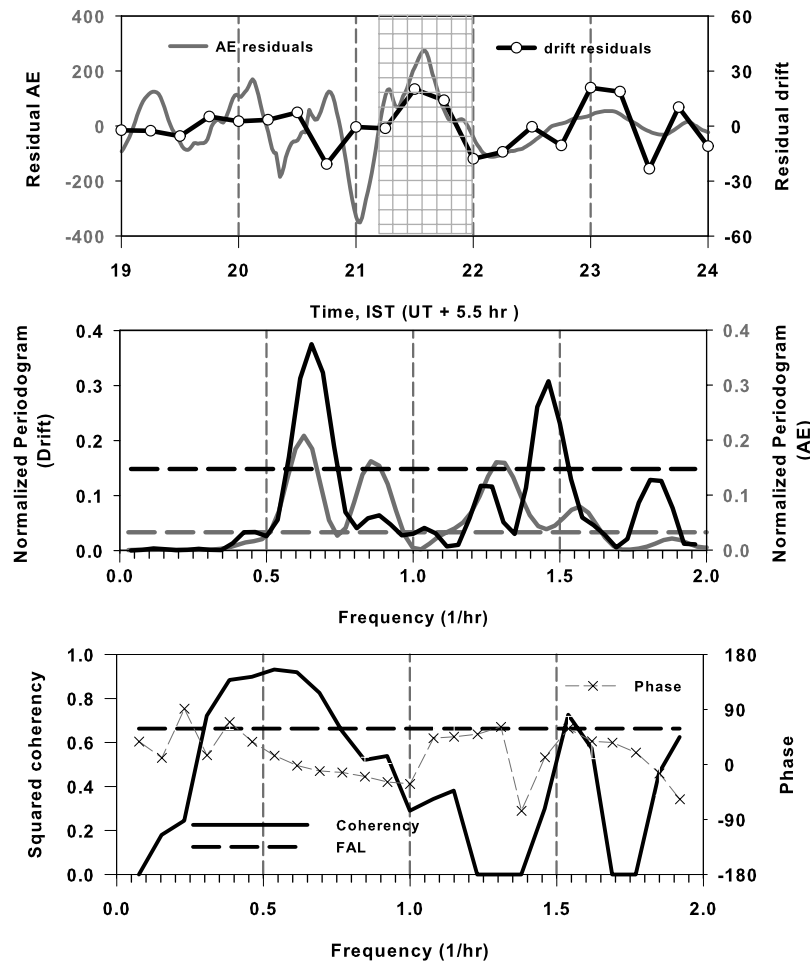


Figure 4. (a) Comparison of AE and drift residuals. The shaded vertical box reveals the in-phase variations of AE and drift residuals during 2110–2200 IST. (b) Normalized periodograms for AE and drift residuals revealing the harmonic components. (c) Coherency and phase spectra.

However, in the absence of significant simultaneous spectral peaks around 1.0 cycle/hr in Figure 3d, the high coherency at this frequency is not considered any further. On the other hand, high coherency at ~ 1.45 cycles/hr (Figure 3e) is also associated with the presence of simultaneous significant spectral peaks in Figure 3d. Moreover, phase spectrum ('+' joined by dashed line) which is overlaid on the coherency spectrum, suggests that the phase relationship between the two residual time series is stable around this frequency. This strongly points towards a consistent causal relationship between IEFy and drift residuals.

[6] Figure 4a reveals the variations in the drift (circles joined by line) and AE (grey line) residuals which do not agree well except during 2110–2200 IST (marked by cross-hatched lines). This is in contrast to the behavior shown in Figure 3c. The harmonic analysis of the two residual time series reveals that the frequency component ~ 0.65 cycle/hr (period ~ 92 min) is “significant” in both the time series (drift in black and AE in grey). This result is different from the result obtained from Figure 3d. However, the coherency spectrum (solid line) reveals a very broad spectral peak at ~ 0.5 cycle/hr which also contains the region of 0.65 cycle/hr. More importantly, the phase spectrum ('x' joined by dashed line) reveals that phase relationship around 0.5 cycle/hr between the two residual time series does not remain

stable indicating the absence of causal relationship between residuals of AE and drift.

3. Discussion

[7] The observation of X-component bay disturbances at low, medium and high latitudes on the nightside as well as the variations in auroral electrojet indices and asymmetric ring current variations clearly suggest the occurrence of substorm activity over the period 1800–2300 IST. Further, the Pi2 burst signatures at the low latitude station, GUAM in the midnight sector (from K. Yumoto and team members, private communications, 2008) substantiate the prevalence of substorms with multiple onsets, particularly beginning at 1931 IST and 2050 IST. In view of these aspects, AE indices during 1800–2300 IST in the present case are taken as primarily representing substorm activity. However, further investigations are needed to understand the underlying physical mechanism responsible for the linear relationship of h/F variation with the variation in the slowly varying component in the AE index during 1800–2300 IST.

[8] One of the most important observations in the present investigation is the in-phase temporal variation of drift residuals with AE residuals (Figure 4a) as well as the out-of-phase variation of drift residuals (Figure 3c) with IEFy

residuals during 2110–2200 IST. The interval 2100–2200 IST corresponds to the last phase of the abnormal ascent and the early part of the rapid descent of the equatorial F layer. The out of phase relationship between drift and IEFy residuals is possibly due to an eastward perturbation electric field. Sudden reduction in IEFy (overshielding condition) can generate eastward electric field perturbations (upward plasma drift) over dip equator at such local times. It is verified that the out-of-phase relationship between IEFy and drift residuals was also noticed in the previous investigations [Chakrabarty *et al.*, 2005, 2006] and one such overshielding event also favored the development of plasma plume during pre-midnight hours [Sekar and Chakrabarty, 2008]. However, the in-phase relationship between drift and AE residuals during the same interval in the present case is striking and is perhaps due to substorm-related intensification of auroral electrojet current systems. The interconnection between the possible pre-midnight overshielding event and the intensification of substorm-related auroral electrojet current system needs to be explored further.

[9] As far as the fast fluctuations in the equatorial vertical drifts are concerned, it is clear that ~ 42 min periodic component in IEFy promptly penetrated into equatorial ionosphere and got imprinted in the zonal electric field variation. Periodicities ~ 30 min and ~ 60 min have been shown to affect [e.g., Chakrabarty *et al.*, 2005] equatorial ionosphere in earlier investigations. However, the present investigation reveals that the fast fluctuations in AE are not temporally coherent with fast fluctuations in the vertical drifts except during 2110–2200 IST when the substorm as well as the overshielding events are present. Further such spectral investigations are needed to understand the effects of storm and substorms on equatorial ionosphere.

4. Summary

[10] Based on a case study, it is demonstrated that a complex interplay of the effects of interplanetary electric field and substorm current systems prevail in the equatorial zonal electric field of the premidnight local time sector during geomagnetic storm strewn with substorms. It is shown that while the variation in the height of the bottom-side equatorial F region ($h'F$) follows the slowly varying component in the auroral electrojet index, AE, the fast fluctuations (period ~ 42 min) in the equatorial F layer vertical plasma drift corresponding to the zonal electric field are mostly controlled by the variations in the interplanetary electric field.

[11] **Acknowledgments.** The authors thank ACE Science Center for the ACE data and WDC-C2 (Kyoto) for the magnetic data. The authors are grateful to K. Yumoto, PI of CPMN, and the team at Kiyushu University for the CPMN data. This work is supported by Department of Space, Government of India.

References

- Chakrabarty, D., R. Sekar, R. Narayanan, C. V. Devasia, and B. M. Pathan (2005), Evidence for the interplanetary electric field effect on the OI 630.0 nm airglow over low latitude, *J. Geophys. Res.*, **110**, A11301, doi:10.1029/2005JA011221.
- Chakrabarty, D., R. Sekar, R. Narayanan, A. K. Patra, and C. V. Devasia (2006), Effects of interplanetary electric field on the development of an equatorial spread F event, *J. Geophys. Res.*, **111**, A12316, doi:10.1029/2006JA011884.
- Earle, G. D., and M. C. Kelley (1987), Spectral studies of the sources of ionospheric electric fields, *J. Geophys. Res.*, **92**, 213.
- Fejer, B., L. Scherliess, and E. R. de Paula (1999), Effects of the vertical plasma drift velocity on the generation and evolution of equatorial spread F, *J. Geophys. Res.*, **104**, 19,859.
- Gjerloev, J. W., R. A. Hoffman, M. M. Friel, L. A. Frank, and J. B. Sigwarth (2004), Substorm behavior of the auroral electrojet indices, *Ann. Geophys.*, **22**, 2135.
- Kelley, M. C., J. J. Makela, J. L. Chau, and M. J. Nicolls (2003), Penetration of the solar wind electric field into the magnetosphere/ionosphere system, *Geophys. Res. Lett.*, **30**(4), 1158, doi:10.1029/2002GL016321.
- Nicolls, J. M., M. C. Kelley, J. L. Chau, O. Veliz, D. Anderson, and A. Anghel (2007), The spectral properties of low latitude daytime electric fields inferred from magnetometer observations, *J. Atmos. Sol. Terr. Phys.*, **69**, 1160.
- Reddy, C. A., V. V. Somayajulu, and C. V. Devasia (1979), Global scale electrodynamic coupling of the auroral and equatorial dynamo regions, *J. Atmos. Terr. Phys.*, **41**, 189.
- Sastri, J. H. (2002), Equatorial geomagnetic and ionospheric effects of substorms, *Indian J. Radio Space Phys.*, **31**, 309.
- Savitzky, A., and M. J. E. Golay (1964), Smoothing and differentiation of data by simplified least squares procedures, *Anal. Chem.*, **36**, 1627.
- Scherliess, L., and B. G. Fejer (1999), Radar and satellite global equatorial F region vertical drift model, *J. Geophys. Res.*, **104**, 6829.
- Schulz, M., and K. Stattegger (1997), Spectrum: Spectral analysis of unevenly spaced paleoclimatic time series, *Comput. Geosci.*, **23**(9), 929.
- Sekar, R., and D. Chakrabarty (2008), Role of overshielding electric field on the development of pre-midnight plume event: Simulation results, *J. Atmos. Sol. Terr. Phys.*, in press.
- Sekar, R., and M. C. Kelley (1998), On the combined effects of vertical shear and zonal electric field patterns on nonlinear equatorial spread F evolution, *J. Geophys. Res.*, **103**, 20,735.
- Subbarao, K. S. V., and B. V. K. Krishna Murthy (1994), Seasonal variations of equatorial spread-F, *Ann. Geophys.*, **12**, 33.
- Taori, A., R. Sridharan, D. Chakrabarty, R. Narayanan, and P. V. S. Ramarao (2001), Co-ordinated thermospheric day-night airglow and ionospheric measurements from low latitudes—First results, *Geophys. Res. Lett.*, **28**(7), 1387.
- Yumoto, K., and the CPMN group (2001), Characteristics of Pi 2 magnetic pulsations observed at the CPMN stations: A review of the STEP results, *Earth Planets Space*, **53**, 981.

D. Chakrabarty and R. Sekar, Space and Atmospheric Sciences Division, Physical Research Laboratory, Navrangpura Ahmedabad-380009, Gujarat, India. (dipu@prl.res.in; rsekar@prl.res.in)

S. Ravindran, Space Physics Laboratory, Vikram Sarabhai Space Center, Thiruvananthapuram- 695022, India. (drsudha56@yahoo.com)

J. H. Sastri, Solar-Terrestrial Physics, Indian Institute of Astrophysics, Bangalore-560034, India. (jhs@iiap.res.in)